soil systems

Supplementary Materials

A comparison of the solubility products of layered Me(II)-Al(III)-hydroxides based on sorption studies with Ni(II), Zn(II), Co(II), Fe(II), and Mn(II)

Lasita Bhattacharya and Evert J. Elzinga *

Department of Earth & Environmental Sciences, Rutgers University, Newark, NJ 07102, USA; lasita.2007@gmail.com
* Correspondence: elzinga@rutgers.edu; Tel.: +1-973-353-5238

Received: 27 February 2018; Accepted: 4 April 2018; Published: date

1. XRD data

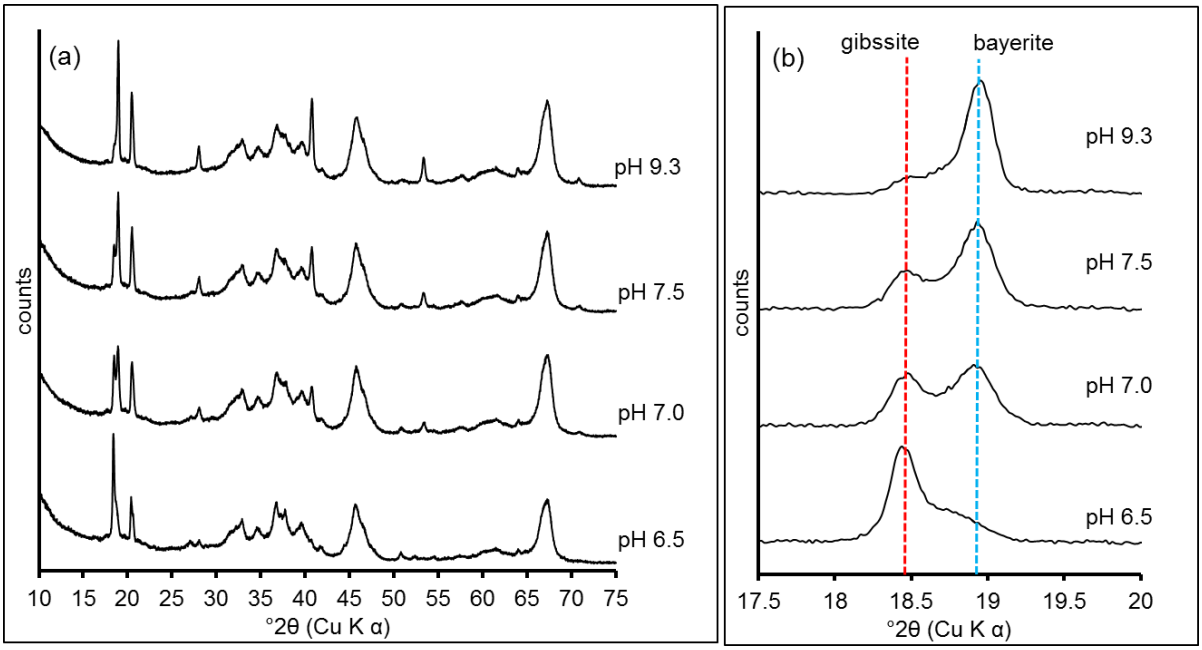

Figure S1. XRD patterns of the γ-Al_2O_3 sorbent following hydration for 2 months in anoxic suspensions with the same particle density (5 g L^{-1}), background electrolyte (0.1 M NaCl), and pH range (6.5-9.3) as used in the sorption studies: (**a**) complete pattern; (**b**) zoom-in of the 17.5-20.0 °2θ range containing reflections indicative of gibbsite and bayerite.

2. XAS analyses

2.1 Data Fitting Procedure

Shell-by-shell fitting of the Me *K*-edge XAS data was done in R-space using WinXAS 3.1 [1]. Theoretical back-scattering paths were calculated using Feff 7.0 [2] in combination with Athena [3]. For Fe, we used the crystal structure of nikischerite (Fe(II)-Al(III)-LDH, characterized in reference [4]) to calculate the theoretical paths. The nikischerite structure was used for the other metals as well, with lattice Fe(II) replaced with Ni(II), Zn(II), Co(II) or Mn(II). Central Me(II) in the LDH structure is surrounded by six first-shell O atoms, and by three Me and three Al second-shell atomic neighbors positioned at the same radial distance. For fitting, the amplitude reaction factor was fixed (the values were 0.9 for Ni and Zn; 0.85 for Co; 0.80 for Fe; and 0.75 for Mn), and a single E_0 shift value was allowed to vary during optimization. Fitting was done with three single scattering paths: first-shell Fe-O, second shell Fe-Fe and second shell Fe-Al. To reduce the number of free parameters, the coordination numbers (N), radial distances (R) and Debye-Waller factors (σ^2) of second-shell Me-Me and Me-Al were constrained to be same, while all other parameters were allowed to vary. Error estimates of the XAS fitting parameters are ± 0.02 Å for the radial distance (R) of the first coordination shells, and ± 0.04 Å for the radial distances of longer shells. For coordination numbers (CN), which are correlated to the Debye–Waller factor, the estimated error is ± 25% for the first shell and ± 40% for the longer shells [5-7].

2.2 Fit Results

Table S1. EXAFS data fitting results of Me(II)–γAl_2O_3 sorption samples and Me(II)–Al(III)–LDH references.

		Atomic Shell										
		Me-O*			Me-Me*			Me-Al*				
Me	sample	N	R(Å)	σ^2 (Å^2)	N	R(Å)	σ^2 (Å^2)	N	R(Å)	σ^2 (Å^2)	Reduced χ^{2**}	E_0
Ni	Ni-Al-LDH	5.4	2.05	0.006	2.6	3.05	0.005	2.6	3.05	0.005	7566	-0.2
	pH 7.00	6.3	2.05	0.006	2.9	3.04	0.007	2.9	3.04	0.007	4328	-0.2
	pH 6.75	5.4	2.05	0.005	1.7	3.04	0.005	1.7	3.04	0.005	3700	1.0
Zn	Zn-Al-LDH	5.8	2.07	0.010	2.2	3.10	0.006	2.2	3.10	0.006	7335	0.8
	pH 7.50	5.7	2.06	0.009	2.9	3.10	0.008	2.9	3.10	0.008	3868	1.4
	pH 7.25	5.4	2.06	0.008	3.3	3.09	0.009	3.3	3.09	0.009	12724	-1.5
	pH 7.00	5.6	2.06	0.009	2.8	3.09	0.009	2.8	3.09	0.009	11576	-0.5
	pH 7.5 (1 mM) #	5.1	2.01	0.013	-	-	-	-	-	-	5059	0.1
Co	Co-Al-LDH	5.9	2.08	0.007	3.2	3.07	0.007	3.2	3.07	0.007	2817	-0.3
	pH 7.75	5.6	2.07	0.006	3.4	3.07	0.008	3.4	3.07	0.008	4418	-1.6
	pH 7.50	5.4	2.08	0.006	2.1	3.08	0.006	2.1	3.08	0.006	1899	-0.7
	pH 7.25	6.4	2.07	0.006	1.8	3.07	0.006	1.8	3.07	0.006	1270	-1.2
Fe	Fe-Al-LDH	5.6	2.14	0.008	3.9	3.14	0.008	3.9	3.14	0.008	4151	1.3
	pH 8.00	5.2	2.11	0.009	3.6	3.13	0.012	3.6	3.13	0.012	1138	0.3
	pH 7.50	5.4	2.12	0.010	1.9	3.12	0.006	1.9	3.12	0.006	4034	1.4
Mn	Mn-Al-LDH	4.9	2.15	0.007	3.0	3.18	0.008	3.0	3.18	0.008	11372	-2.0
	pH 9.25	5.6	2.15	0.007	2.6	3.20	0.007	2.6	3.20	0.007	1641	-0.3
	pH 9.00	6.1	2.16	0.009	4.2	3.19	0.010	4.2	3.19	0.010	1329	-0.3
	pH 8.75	5.4	2.17	0.007	2.5	3.20	0.010	2.5	3.20	0.010	8434	-1.3

*N is coordination number, R is radial distance, and is Debye-Waller factor. Error estimates are provided in SI section 2.1 above; ** Reduced χ^2 as defined in Ressler [1]; # For the 1.0 mM Zn sample only the O shell was fitted.

3. Solution chemical and thermodynamic data

Table S2. Summary of the solution chemical and thermodynamic data used to calculate *K*sp of the Me(II)-Al(III)-LDH phases formed in the equilibrated sorption samples (*Table S2 continues on next page).*

Calculation Results [a]	**Ni**		**Zn**						**Co**			**Fe**		**Mn**		
pH (initial)	6.75	7.00	7.00 (1mM)	7.25 (1mM)	7.50 (1mM)	7.00 (3mM)	7.25 (3mM)	7.50 (3mM)	7.25	7.50	7.75	7.50	8.00	8.75	9.00	9.25
$[Me(II)]_{tot}$ (mol/L)	$9.51*10^{-5}$	$4.19*10^{-5}$	$2.11*10^{-4}$	$7.46*10^{-5}$	$3.02*10^{-5}$	$7.05*10^{-4}$	$2.16*10^{-4}$	$8.78*10^{-5}$	$2.32*10^{-4}$	$9.05*10^{-5}$	$3.56*10^{-5}$	$2.58*10^{-4}$	$4.39*10^{-5}$	$2.59*10^{-4}$	$1.33*10^{-4}$	$4.10*10^{-5}$
$[Me^{2+}]$ (mol/L)	$9.38*10^{-5}$	$4.13*10^{-5}$	$1.90*10^{-4}$	$6.69*10^{-5}$	$2.69*10^{-5}$	$6.35*10^{-4}$	$1.94*10^{-4}$	$7.88*10^{-5}$	$2.28*10^{-4}$	$8.90*10^{-5}$	$3.49*10^{-5}$	$2.51*10^{-4}$	$4.24*10^{-5}$	$2.47*10^{-4}$	$1.26*10^{-4}$	$3.74*10^{-5}$
$[MeCl^{+}]$ (mol/L)	$1.20*10^{-6}$	$5.50*10^{-7}$	$1.96*10^{-5}$	$6.84*10^{-6}$	$2.73*10^{-6}$	$6.52*10^{-5}$	$1.98*10^{-5}$	$7.98*10^{-6}$	$3.61*10^{-6}$	$1.40*10^{-6}$	$5.43*10^{-7}$	$5.56*10^{-6}$	$9.39*10^{-7}$	$8.86*10^{-6}$	$4.49*10^{-6}$	$1.32*10^{-6}$
pH [b] (equilibrium)	6.70	6.93	6.84	7.15	7.39	6.50	6.83	7.09	7.08	7.36	7.59	7.37	7.88	8.59	8.79	9.13
$[Cl^{-}]$ (mol/L) [c]	0.097	0.097	0.097	0.097	0.097	0.097	0.097	0.097	0.097	0.097	0.097	0.097	0.097	0.097	0.097	0.097
$[Na^{+}]$ (mol/L)[d]	0.116	0.103	0.103	0.106	0.109	0.103	0.106	0.109	0.106	0.109	0.113	0.110	0.109	0.101	0.103	0.106
Ionic strength	0.117	0.103	0.103	0.106	0.109	0.103	0.106	0.109	0.106	0.109	0.113	0.110	0.109	0.101	0.103	0.106
Activity coefficient (γ) for univalent ions	0.77	0.78	0.78	0.78	0.78	0.78	0.78	0.78	0.78	0.78	0.77	0.78	0.78	0.78	0.78	0.78
Activity coefficient (γ) for divalent ions	0.36	0.37	0.37	0.37	0.36	0.37	0.37	0.36	0.37	0.36	0.36	0.36	0.36	0.37	0.37	0.37
(Al^{3+}) $e_{gibbsite}$ (mol/L)	$4.37*10^{-13}$	$9.23*10^{-14}$	$1.66*10^{-13}$	$1.95*10^{-14}$	$3.72*10^{-15}$	$1.74*10^{-12}$	$1.78*10^{-13}$	$2.95*10^{-14}$	$3.09*10^{-14}$	$4.47*10^{-15}$	$9.33*10^{-16}$	$4.27*10^{-15}$	$1.26*10^{-16}$	$9.33*10^{-19}$	$2.34*10^{-19}$	$2.24*10^{-20}$
$(Al^{3+})e_{bayerite}$ (mol/L)	$7.25*10^{-12}$	$1.53*10^{-12}$	$2.75*10^{-12}$	$3.24*10^{-13}$	$6.17*10^{-14}$	$2.88*10^{-11}$	$2.95*10^{-12}$	$4.90*10^{-13}$	$5.14*10^{-13}$	$7.41*10^{-14}$	$1.55*10^{-14}$	$7.08*10^{-14}$	$2.09*10^{-15}$	$1.55*10^{-17}$	$3.89*10^{-18}$	$3.72*10^{-19}$
Ksp (gibbsite)[f]	$8.39*10^{-23}$	$8.53*10^{-23}$	$1.90*10^{-22}$	$1.93*10^{-22}$	$1.79*10^{-22}$	$1.94*10^{-22}$	$1.88*10^{-22}$	$1.84*10^{-22}$	$3.62*10^{-22}$	$3.69*10^{-22}$	$3.43*10^{-22}$	$7.59*10^{-22}$	$7.51*10^{-22}$	$1.27*10^{-20}$	$1.28*10^{-20}$	$1.25*10^{-20}$

Average Ksp (gibbsite)	$8.46(\pm0.1)\times10^{-23}$		$1.89(\pm0.07)\times10^{-22}$			$1.89(\pm0.05)\times10^{-22}$			$3.58(\pm0.13)\times10^{-22}$			$7.55(\pm0.06)\times10^{-22}$		$1.27(\pm0.02)\times10^{-20}$		
Ksp (bayerite)[f]	$2.14*10^{-22}$	$2.17*10^{-22}$	$4.83*10^{-22}$	$4.93*10^{-22}$	$4.57*10^{-22}$	$4.94*10^{-22}$	$4.79*10^{-22}$	$4.69*10^{-22}$	$9.25*10^{-22}$	$9.40*10^{-22}$	$8.75*10^{-22}$	$1.94*10^{-21}$	$1.91*10^{-21}$	$3.24*10^{-20}$	$3.28*10^{-20}$	$3.19*10^{-20}$
Average Ksp (bayerite)	$2.16(\pm0.02)\times10^{-22}$		$4.78(\pm0.18)\times10^{-22}$			$4.81(\pm0.12)\times10^{-22}$			$9.13(\pm0.34)\times10^{-22}$			$1.93(\pm0.02)\times10^{-21}$		$3.23(\pm0.04)\times10^{-20}$		

[a] [ ] and ( ) denote concentration and activity, respectively; [ ]*γ=( ).

[b] pH measured at equilibrium and used in the calculation of Ksp.

[c] $[Cl^-]$ equals the NaCl concentration used to control the ionic strength of the system.

[d] $[Na^+]$ is derived from the NaCl background electrolyte as well as from the NaOH used as a pH titrant .

[e] (Al^{3+}) was calculated assuming equilibrium with either gibbsite or bayerite.

[f] Ksp values calculated based on equation 2 in the main text, assuming equilibrium with either gibbsite or bayerite .

4. References

1. Ressler, T. WinXAS: A new software package not only for the analysis of energy-dispersive XAS Data. *J. Phys. IV France* **1997**, *7*, C2–269.
2. Ankudinov, A. L.; Rehr, J. J. Relativistic calculations of spin-dependent X-ray absorption spectra. *Phys. Rev. B* **1997,** *56*, R1712–R1715.
3. Ravel, B.; Newville, M. ATHENA, ARTEMIS, HEPHAESTUS: data analysis for X-ray absorption spectroscopy using IFEFFIT. *J. Synchrotron Radiat.* **2005**, *12*, 537–541.
4. Huminicki, D. M. C.; Hawthorne, F. C. The crystal structure of nikischerite, $NaFe^{2+}{}_6Al_3(SO_4)_2(OH)_{18}(H_2O)_{12}$, a mineral of the shigaite group. *Can. Mineral.* **2003**, *41*, 79–82.
5. Elzinga, E. J.; Sparks, D. L. Reaction condition effects on nickel sorption mechanisms in illite–water suspensions. *Soil Sci. Soc. Am. J.* **2001**, *65*, 94–101.
6. Elzinga, E. J.; Sparks, D. L. Nickel sorption mechanisms in a pyrophyllite–montmorillonite mixture. *J. Colloid Interface Sci.* **1999,** *213*, 506–512.
7. Zhu, Y.; Elzinga, E. J. Formation of layered Fe(II)-hydroxides during Fe(II) sorption onto clay and metal-oxide substrates. *Environ. Sci. Technol.* **2014**, *48*, 4937–4945.